Chapter 2
Synthesis and Characterization of TiO_2–Cr Thin Films

Abstract Details of the important experimental conditions of the synthesis of Cr doped TiO_2 thin films by means of co-deposition by magnetron sputtering process are presented. Furthermore, a brief description of the structural, electrical and optical characterizations set-up is provided. These physical characterizations are based on X-ray diffraction, atomic force and scanning electronic microscopy, LBIC… techniques.

Keywords Chromium–Doped TiO_2 · Magnetron sputtering method · Chemical etching · Physical characterization setup

In this chapter, the experimental methods and the experimental condition of the synthesis and characterization of TiO_2–Cr thin films have been detailed. The used fabrication processes are the co-deposition by magnetron sputtering and the electrochemical attack technique. We also give a brief description the structural, electrical and optical characterizations setup.

2.1 Synthesis of Thin Films by Magnetron Sputtering

The sputtering is one of the most used techniques for the preparation of the semiconductor metal oxides thin films. This technique allows both qualitative and quantitative control of the thin films deposition. The deposition experimental setup is presented in Fig. 2.2, it consists of an argon vacuum chamber, equipped with a system target-magnetron door and heated stage. This apparatus is powered by a radio frequency generator. Under the action of electric field applied by the radiofrequency generator, argon atoms are ionized and accelerated inside the target electric field. The target has a negative voltage compared to the argon plasma. The pulverized particles tend to be electrically neutral and distributed in the chamber. A number of them are collected onto a substrate placed in front of the target, and on which thin film is grown.

© The Author(s) 2015

A. Hajjaji et al., *Chromium Doped TiO_2 Sputtered Thin Films*,
SpringerBriefs in Manufacturing and Surface Engineering,
DOI 10.1007/978-3-319-13353-9_2

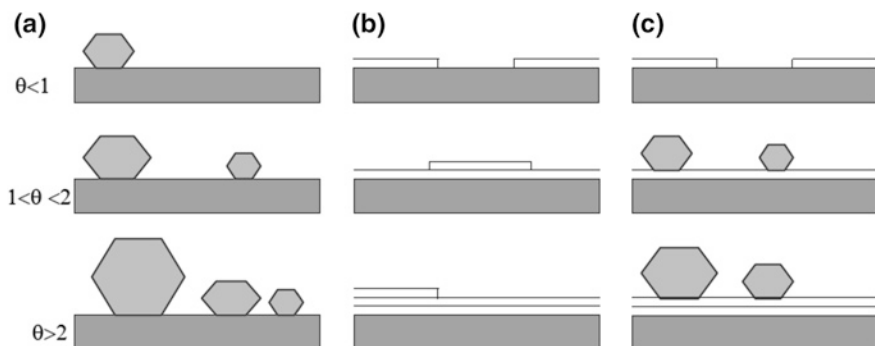

Fig. 2.1 The different modes of thin film growth

2.1.1 The Thin Film Formation Steps

2.1.1.1 Classification of the Growth Modes

In a simple approach, we class the thin films growth on a substrate into three categories [1] schematically illustrated in Fig. 2.1:

(a) **Patches growth (Volmer-Weber (VW) mode)**
In this growth mode, patches are formed on a substrate surface by clusters nucleation, Fig. 2.1a. This growth will take place when atoms or molecules, arriving on the substrate surface, have more affinity to bind together than to the substrate. Therefore, it is three-dimensional growth: a typical case of this growth is that of metal films on insulator substrates.

(b) **Layers growth (Franck-Van der Merwe (FM) mode)**
This growth mode takes place when the atom-substrate interaction is very strong. The first atoms arriving on the substrate surface condense and form a single layer covering the entire substrate area, Fig. 2.1b: there is a two-dimensional nuclei growth to form a layer, and so on layer by layer.

(c) **Mixed growth (Stranski-Krastanov (ST) mode)**
This growth mode is an intermediate case between the two previous modes (VW and FM modes): the growth is primarily two-dimensional to form the first thin film layer; However, as the energy of atom-substrate interaction gradually decreases, growth tends to become three-dimensional with patches formation, Fig. 2.1c.

2.1.1.2 The Morphology of Thin Films

The thin film morphology depends on different basic parameters as: the adsorption energy of deposited elements, their possible interaction with the substrate atoms, their mobility on the surface, sputtering rate, thermal diffusion, temperature, etc.

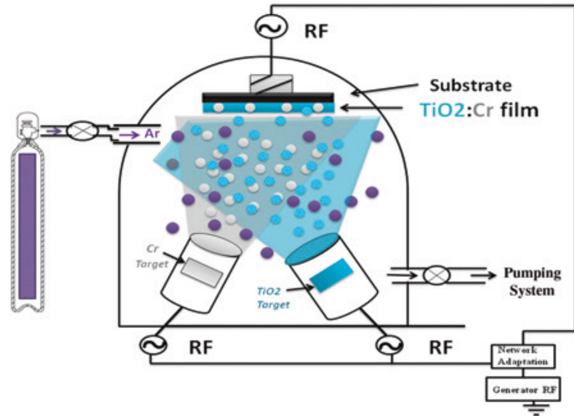

Fig. 2.2 System co-deposition by magnetron sputtering

2.1.2 Principle of Operation

2.1.2.1 Description of the Deposition Machine

The used deposition chamber consists on a CMS-18 reactor including three sputtering posts. Co-disposition by magnetron sputtering system is schematized in Fig. 2.2.

Before the plasma switch on, the system must be pumped to reach a vacuum of order 10^{-5} mTorr. To produce the discharge, a partial pressure of high purity argon equals to 1.2 mTorr is created in the chamber. Targets can then be turned on individually, thus creating two independent plasma sources. The power of each RF sources is then adjusted within a range between 8 and 360 W depending on the desired composition.

2.1.2.2 Deposition Requirements for the Development of Cr-Doped TiO_2 Thin Films

Cr-doped TiO_2 thin films have been developed by cathodic radiofrequency magnetron sputtering of two targets: TiO_2 and chromium (Cr). Purity index of the two targets are 99.995 and 99.99 % for titanium dioxide and chromium, respectively. The applied power to the target, the pressure, flow and volumetric ratio of Ar and O_2 gases, as well as the possible polarization of the substrate are chosen based on the results of previous work (Table 2.1).

2.1.2.3 Drawbacks and Benefits

(a) **Benefits**

- Deposition of all types of materials: refractory metal (W, Ta, Mo, …), alloys, oxides, dielectrics.
- Good adhesion.

Table 2.1 Deposition conditions used for the preparation of thin films of TiO_2

Power applied to the TiO_2 target (W)	Power applied to the Cr target (W)	Ar flow (sccm)	O_2 flow (sccm)	Pressure (mTorr)
360	8	80 %	20 %	1.2
//	15	//	//	//
//	25	//	//	//
//	50	//	//	//
//	100	//	//	//
//	150	//	//	//

- Good uniformity of thickness if target diameter $\gg$ substrate diameter.
- This method allows getting large surfaces films.

(b) **Drawbacks**

- More expensive equipment and more difficult to implement compared to evaporation technique.
- The deposition is made under an inert atmosphere (Argon). The resulting film is not crystalline as in the vacuum deposition case.
- Defects are created in layers by energetic particles and plasma UV photons.

2.1.2.4 Conclusion

Magnetron sputtering is less efficient than the CVD process due to deposition velocity. However, its implementation is simpler and can remove any solid material at ordinary temperature. In addition, magnetron sputtering technique allows deposition of insulating layers as well as metallic layers (aluminum, chrome …). It is therefore widely used for the realization of interconnection layers in integrated devices.

2.2 Electroetching

For the development of thin layers of porous silicon (PS), we used the conventional technique of electrochemical anodization (AE). It takes place in a wet environment based hydrofluoric acid (HF). This technique consists of the silicon substrate to attack the anode of an electrochemical cell. During the attack, a fixed current flows between the anode (the starting substrate) and the cathode (gold or platinum).

2.2.1 Cell Anodizing

Thin films are produced in a cell comprising a single reservoir Teflon (Fig. 2.3). During the formation of SP, the rear face of the Si substrate acts as anode (it is connected to the positive pole of the power supply). Its front face (polished surface) is contacted with the electrolytic solution is maintained at a negative electrical

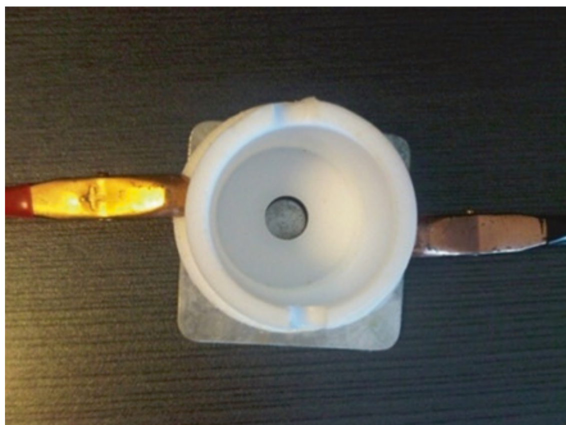

Fig. 2.3 Electroetching

potential relative to the rear face. The rear contact is ensured by moderate pressure on a plate stainless aluminum.

The sealing of the silicon wafer is provided by an O-ring which delimits the area of formation of the PS (about 4 cm^2). The cell is connected to a potentiostat used as current source. A computer serves to control the variation of the anodization current.

2.2.2 *Development of the PS Layers*

Before the formation of the PS, the substrate is degreased. For this, the sample is rinsed successively in a solution of acetone and deionized water. These rinses help remove dust and organic origin of the surface of the substrate particles. To improve the homogeneity of the layers, an ohmic contact Si/Al on the back is made. The procedure consists of depositing an Al layer by evaporation on the rear face of the silicon wafer, followed by drying in an infrared oven under a nitrogen stream and baked for 15 min at a temperature of 550 °C [2]. The porous structures are obtained from a single silicon substrate or polycrystalline P-type, boron doped, orientation (100), respectively resistivity 1–3 Ω cm and 5–2 Ω cm having a thickness of order of 500 and 330 microns. The porous layers have a circular area of about 4 cm^2. The electrochemical etching is performed in hydrofluoric acid, HF (40 %) diluted in ethanol with 1:4 as ratio.

2.3 Microstructural and Analytical Characterization

In this section, we present the characterization techniques used to understand the microstructure and composition of thin-film-type TiO_2–Cr obtained by magnetron sputtering.

2.3.1 X-ray Photoelectron Spectroscopy (XPS)

X-ray photoelectron spectroscopy is a technique of surface analysis to obtain information about the nature of chemical bonds in the films as well as their elemental composition. Thus, when a thin film is exposed to X-ray photons, atoms that compose these interact with photons. This energy ratio leads to the expulsion of some of the electrons of the atoms constituting the heart layer, the electrons leave the atom with a specific kinetic energy. This, combined with the nature of the material concerned, can determine the distance traveled by the photoelectrons expelled by the X-ray. In case the average path can reach the surface of the film, they are extracted from the material and pass into the void where they are then collected by a system of magnetic lenses and/or to guide them to electrostatic spectrometer. They can then be counted and classified according to their kinetic energy, which is closely linked to their binding energy:

$$h\nu = E_L + E_C + W \tag{2.1}$$

Thus, since the photon energy hv X incidents and the work function W are known energy EL binding the electron can be deduced.

As part of this work, we used a VG 220i-XL Escalab device VG Instruments, the vacuum base is 10^{-10} Torr, combined with a hemispherical detector. Al kα a monochromatic source (1486.6 eV) and Mg kα (1253.6 eV) permit analysis of orbital Ti 2p, 2p Cr, O1s CasaXPS using the software and before and after cleaning the surface of the films by spraying by means of a beam of Ar^+ ions to 5 keV.

2.3.2 Infrared Fourier Transform Spectroscopy (FTIR)

This technique allows us to study the nature of chemical bonds in a material. For this purpose, the infrared frequencies (energy) absorbed by the chemical bonds of the molecules present in the sample are measured. These bonds have different modes of vibration corresponding to wavelengths specific infrared wavelengths, working in a wide frequency range to identify the types of bonds present in the film. In practice, if we work in transmission mode, the sample is exposed to an infrared transmitted beam which passes through an interferometer, a signal is then obtained as an interferogram. A Fourier transform of this signal is performed, resulting in a frequency spectrum. A first measurement is performed on a blank substrate (no deposit) and then the sample (thin film + substrate). For FTIR measurements, we used a Nicolet 6700 FT-IR unit of Thermo Electron Corporation, to vary the wavelength of far-infrared to the UV-Visible (400–4,000 cm^{-1}). The test chamber is constantly purged with ultra-dry air, which eliminates the absorption of water modes.

2.3.3 Grazing Incidence X-ray Diffraction (GIXRD)

The classical method of X-ray analysis typically involves an X-rays penetration depth from the micrometer to millimeter rang. Thus, measurements of X-ray diffraction (XRD) in the classic configuration θ–2θ are generally less adapted to the c of the deposited thin films crystalline structure (risk of interference with the substrate XRD diagram). For these reasons, measurements of X-ray diffraction are done with grazing incidence angle θ between the incident beam and the sample surface (on the order of 1°) [3]. Therefore, the irradiated depth decreases and the length of the X-ray path in the thin layer increases laterally, which allows to an increase in the intensity of the signal from the thin film. In this configuration, the incident angle θ remains fixed while the detector of the diffracted X-ray is mobile in 2θ (angle of deviation).

For our GIXRD measures, we used a PW3040/60 X pert Pro diffractometer from Philips equipped with a Cukα (1,543a) source, the incidence beam angle θ is set to 0, 5°. The different analyses were used to study different crystalline structures of the deposited thin film, and estimate crystallite size. The crystallites size is reached by the Scherrer relation (Eq. 2.2), or the average crystallite size d can be estimated by considering the source wavelength (λ), FWHM of the peak (Δ), and the tilting angle (2θ); all adjusted by a correction factor (k), usually in the range of 0.9 [4].

$$d \simeq \frac{0.9\lambda}{\Delta(2\theta)\cos\theta} \tag{2.2}$$

2.3.4 X-ray Reflectometry (XRR)

This technique has also been used to determine precisely the density and thickness of deposited thin films. In this case, the incident beam is launched with grazing incidence angle (θ) with the sample surface and a detector is used to measure the specular reflective intensity.

2.3.5 Atomic Force Microscopy (AFM)

The atomic force Microscopy (AFM), belongs to the family of near-field microscopes. This technique was developed in 1986 by Binning et al. The operation of the AFM is based on the interaction between a tip and the studied surface. The atomic force microscope (Fig. 2.4) operates at air, vacuum and also in liquid medium, which permits its use in various fields such as electrochemistry and biology. The sensitivity of its tip to different types of interaction, which can be controlled, allows in addition to surfaces imaging, measurements of several properties as: elasticity, viscosity, mechanical tribological (friction, adhesion), magnetic and electric, with a resolution of the order of nanometer and this for practically any type of sample.

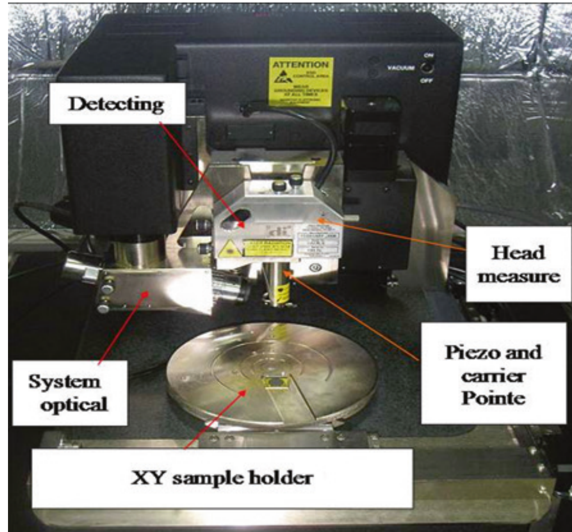

Fig. 2.4 Photograph of the AFM Veeco Instruments, which is at the center of technological resources (Technopolis Borj Cedria)

(a) **Equipment**

The AFM used (Fig. 2.4) to characterize our samples is an multimode Nanoscope III (Veeco Instruments) AFM. This device can be operated in 'contact' mode or "tapping" mode. The central element is the probe, it is a lever on which a nanometric tip is mounted. This tip is in mechanical contact with the surface to determine its morphology. Through a piezoelectric tube, the tip can be moved in X, Y and Z directions. The interaction between the tip and the surface is characterized by the measure of a physical data of the lever as: its deflection and amplitude of vibration. This measure is in most cases done by sending a laser beam at the back of the lever and detecting the reflected beam (Fig. 2.5). A control system of the tip maintains constant interaction strength, allowing to reconstruct point by point the topology of the surface. The regulation of the peak altitude is made by comparing the measured signal to the control signal. The error signal is then returned to the piezoelectric system and the peak altitude is then changed.

(b) **Different AFM operating modes**

«Contact» mode: when the tip and the sample is continuously in contact, the strength of interaction is responsible of the lever deflection on a quasi-static way. Most of the topographic images are obtained with this operating mode. The multimode AFM software contains algorithms that measure and present results as: cross-section analysis, roughness measurement, particle size analysis, depths analysis, the spectral density of the pattern, histogram analysis, forces measurement …

'Tapping' mode: tapping is the most used mode for the study of rough surfaces. In fact, it avoids degradation of the tip, friction and displacement of material from the surface of materials, since the interaction strength is

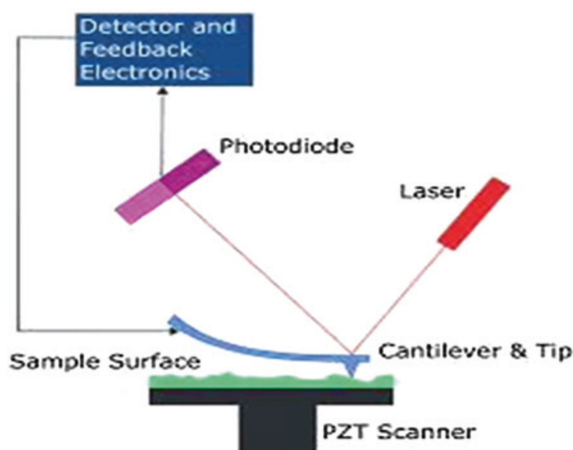

Fig. 2.5 Operating principle of a atomic force microscope (AFM)

normal to the surface (no tangential component). Due to the high vibration frequencies of the tip that hits the surface of the sample intermittently, it also allows to minimize the effects of capillary action taking place in the presence of water film. For these reasons, we have used this mode for morphological studies of TiO_2 thin films.

2.3.6 Scanning Electron Microscope (SEM)

The scanning electron microscope (SEM) is used to get the microscopic images of a sample in vacuum with an electrons beam (typically between 5–25 keV energy). Under the effect of the electron, sample is the seat of a large number of physical phenomena (excitation of plasmons, emission of electrons …). In a conventional microscope, sensor and electron gun are in the same side of the sample. The most detected phenomena is the emission of secondary electrons. Those are the ejected electrons from the sample by the primary electrons beam having energy less than 50 eV. Backscattered electrons can also be detected. These are the primary beam electrons that have sufficiently deflected from their initial trajectory to sample out of elastic or quasi-elastic collisions, without energy transfer. Their energy is then so close to the primary beam energy. The achieved images represent essentially a topographic contrast. Indeed, the emission depth of secondary electrons is less than 10 nm. In addition, the number of emitted electrons depends on the ‘shape’ of the surface and the detected number depends on its orientation from the detector and the gun. Backscattered electron images are sensitive to the atomic number of the elements but the topographic contrast is less good. The scanning microscopes are often equipped with an energy dispersive spectrometer (EDX, “Energy Dispersive X-ray spectrometer”). In this work, the SEM analyses were performed at INRS-EMT by means of a JEOL JSM 7401F microscope.

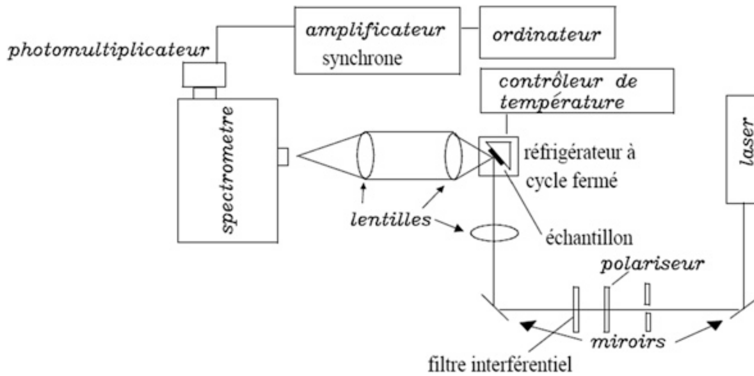

Fig. 2.6 Principle of operation of the assembly photoluminescence

2.3.7 Photoluminescence Setup

The experimental set-up is shown in Fig. 2.6. An ionized Argon laser ($\lambda = 488$ nm) is used to excite the sample which is placed in vacuum. The light emitted from the sample is focused by two lenses system at the entrance of a spectrometer equipped with a GaAs photomultiplier cooled with water. The current given by the photomultiplier is converted to voltage (by a resistors box) which is measured using a synchronized detection itself connected to a computer. The synchronized detection used requires an excitation beam chopped at a fixed rate.

2.4 Electrical and Optoelectronic Characterizations

2.4.1 Test of Gas Sensors

The chosen sensor element is TiO_2 thin film of ~50 nm thick. In order to test this sensor, gold electrodes closely spaced (3 mm) are deposited on this film by evaporation. The TiO_2-based gas sensor is placed in a Chamber where variation of conductivity is measured with different gas concentration, by controlling the temperature of the sample from ambient to 300 °C. The heating elements and the thermocouple are connected to a temperature controller. Figure 2.7 shows the whole experimental set-up used to test gas sensors. All measures devices are connected to a computer via an 'Agilent Technologies' GPIB card that allows simultaneous interfacing of up 14 devices. The measurements are controlled through programs developed with the HP VEE programming language.

An HP 4140B pico-ammeter [5] is used for the conductivity measurement in static regime. HP4140B (Fig. 2.8) allows doing three types of measures simultaneously:

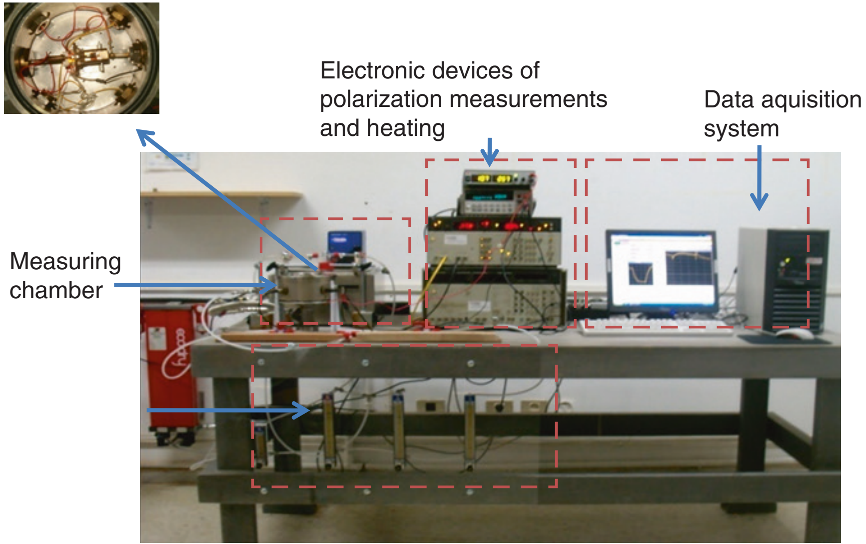

Fig. 2.7 Diagram of the tester to IPEST [8]

Fig. 2.8 Pico-ammeter HP4140B

- conductance versus temperature: G (T).
- the conductance versus time at constant temperature: G (t),
- The current-voltage characteristics: I (V)

The sensors responses are visualized in real time. The conductance dependency on time and temperature changes was treated with the following procedures: isotherm and temperature cycles. An image of the program interface is shown in Fig. 2.9.

2.4.2 Light Beam Induced Current Technique (LBIC)

About 90 % of photovoltaic electricity is produced from mono and multicrystalline silicon cells. Knowledge of the diffusion length (or life time) of minority carriers in Silicon used in the development of solar cells is necessary in order to

Fig. 2.9 Image of the interface of the program acquisition and temperature control based on time

adapt and optimize fabrication processes. The aim of the LBIC technique is the diffusion length measurement and the lifetime of minority carriers in mono and multicrystalline Silicon. LBIC technique measures the variation of the induced current at the terminals of a photovoltaic cell under monochromatic illumination (laser) focused at a point of a few µm in diameter. Minority carriers are photo-generated in a given point on the surface of the cell, producing the LBIC current. The LBIC current measurement enables to calculate the diffusion length of minority carriers. Figure 2.10 shows the LBIC set-up. The multicrystalline Silicon cell is mounted on motorized x y z stage. The x and y motors provide lateral movement of the sample compared to focused and fixed laser spot. The z motor is used to focus the laser on the diode surface. The sample is fixed on the x y z motorized stage with vacuum pump. The short-circuit current collected at the terminals of the cell is converted, amplified and filtered by a synchronized detection. At the output of the synchronized detection, the signal passes through a digital Voltmeter to a microcomputer using an IEEE cable. Once the value of the LBIC current registered, the microcomputer controls the motor in x (or in y) to change the position of the diode with the incident laser for a new LBIC measure. In this experiment, the red (He–Ne) laser of wavelength 628 nm is used.

The principle of measurement is illustrated in Fig. 2.11.

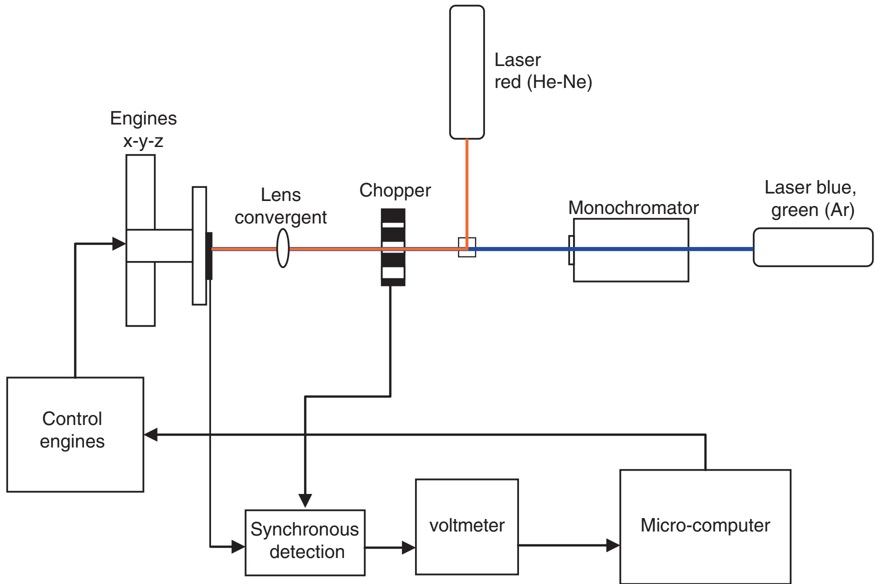

Fig. 2.10 Schematic assembly for measuring the current LBIC [9]

Fig. 2.11 A test structure for measuring the current in the case of LBIC cell multicrystalline Si treated PS. LBIC current measurement to estimate the diffusion length of minority carriers

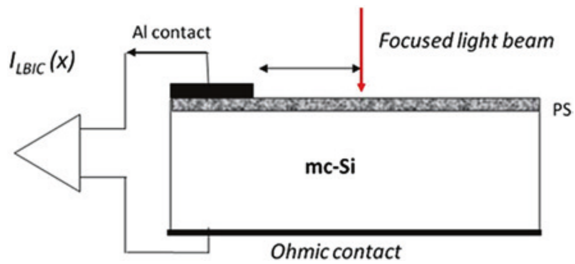

2.4.3 *Quantum Efficiency*

The quantum efficiency gives information on the overall performance of the structure. The external quantum efficiency at a given energy is the ratio of the number of collected carriers on number of incident photons. If each photon of a specific wavelength generates a collected charge carrier, the quantum efficiency is unity. As it is noted earlier, the Silicon absorption coefficient varies with the wavelength of the radiation. The photons with low wavelength are absorbed close to the surface (to area of the transmitter of the cell) while those with high wavelength are

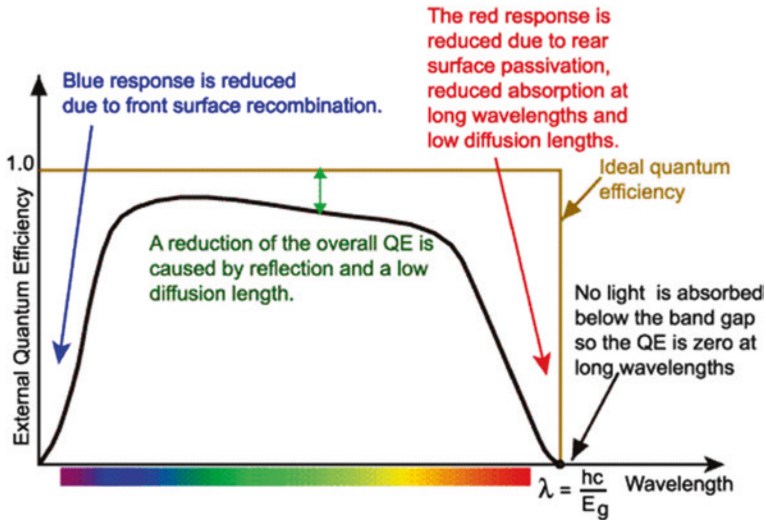

Fig. 2.12 External quantum efficiency of a solar cell [10]

absorbed more in depth into the device (at the level of the base). We can therefore access the spectral behaviour and the efficiency of each region constituting the cell. This parameter can be affected by several factors: the surface and bulk recombination phenomena play an important part. Reflection on the front and the low diffusion length of carriers lead to decreasing the quantum efficiency on the overall wavelengths range (Fig. 2.12). The presented parameter does not take into account optical losses as reflection or transmission through the cell: it is the external quantum efficiency (EQE). We can correct the quantum efficiency by considering only the absorbed photons, in this case we take into account losses by reflection: it is the internal quantum efficiency (IQE) which takes into account only the specific characteristics of the cell (diffusion length, surface and volume recombination).

2.5 Optical Characterisations

2.5.1 UV-Visible Spectrometer

UV-visible spectrophotometry is a characterization technique to reach the optical properties (transmission and reflectivity) of the materials. The measurements are performed on a wide wavelength range from 175 nm (UV) to 3,300 nm. The spectrometer is equipped with an integrating sphere which allows us to take into account the backscattered light (Fig. 2.13) [6]. The entire light incident in any direction to this highly reflective walls sphere is perpendicular reflected to detectors located on the wall of this sphere.

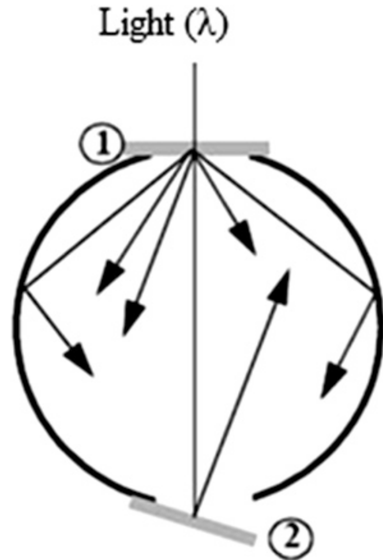

Fig. 2.13 Diagram of the integrating sphere used

The measurement of the total transmission (T) is performed by placing the sample at the entrance of the sphere (position (1), Fig. 2.13), the light that comes from a polychromatic source first penetrate the sample. The transmitted part is collected by a detector located on the surface of the sphere. The reflection is measured by placing the sample at position (2) (Fig. 2.13). The R(λ) and T(λ) measurement are performed using a lambda 950 spectrometer, equipped with an integrating sphere (150 mm or PELA 1021 infra gold) which allows to take into account the backscattered light.

2.5.2 Ellipsometry

Ellipsometry is an optical technique for surface analysis based on the measurement of the change in the state of polarization of the light after reflection on a flat surface. This technique, which the principle was discovered a century ago, knows a great success since 20 years thanks to the use of computing and electronic control of the motor, allowing optimization of measures.

(a) **Principle of measurement** [7]

Consider a plane wave arriving on a flat surface. Part of the wave is transmitted or absorbed through the surface, another part is reflected by the surface (Fig. 2.14). In this work, we consider only to the reflected part. The incident wave can be decomposed along two axes:

- one parallel to the incidence plane
- the other perpendicular to the incidence plane.

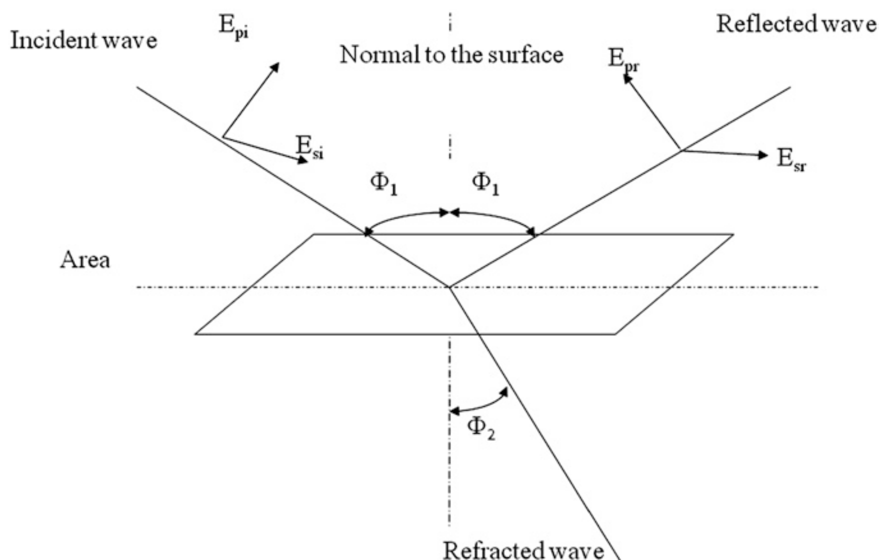

Fig. 2.14 Reflection of the polarization axes in the surface of the sample

The used index are: p for parallel, s for perpendicular, i for incident. The change of the electric field after reflection on the sample can be represented by two factors acting on each of the field components:

- the reflection coefficient of the sample for polarization parallel to the incidence plane is:

$$r_p = E_{pr}/E_{pi} = |r_p| \exp(j\delta_p) \tag{2.3}$$

- the reflection coefficient of the sample for polarization perpendicular to the incidence plane:

$$r_s = E_{sr}/E_{si} = |r_s| \exp(j\delta_s) \tag{2.4}$$

Both r_p and r_s coefficients are complex. Their modules $|r_p|$ and $|r_s|$ represent the variation of the field component amplitude, and their phases δp and δs, represent the delay introduced by the reflection. In practice, the measured is the ratio of these two factors, which is expressed in the following form:

$$r_p/r_s = \tan\psi \exp(j\Delta) = \rho \tag{2.5}$$

ρ measurement leads to the identification of two quantities (ψ and Δ, or tan ψ and cos Δ). A measurement at a given wavelength and incidence angle will allow the calculation of the index n and k of a substrate knowing the thickness of the layer, or the index n and thickness e of a layer knowing extinction coefficient k. Finally,

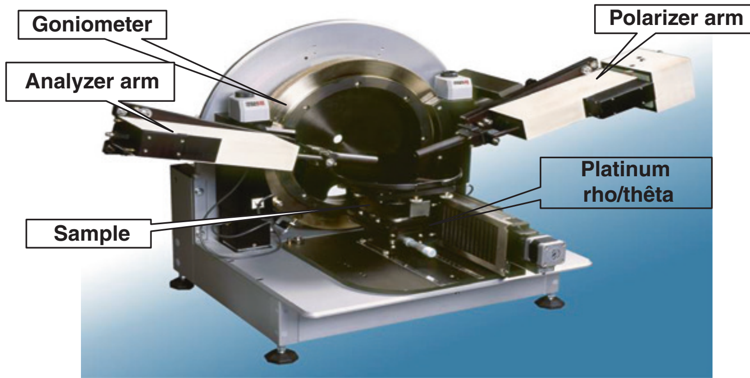

Fig. 2.15 SOPRA GES5 spectroscopic ellipsometer

the previous relationships allow us to determine some optical characteristics such as refractive index, extinction coefficient and absorption coefficient.

(b) **Experimental setup**

The used device is a rotating polarizer ellipsometer (model GES5 de SOPRA, Fig. 2.15).

This Ellipsometer is composed of a source arm and detection arm that can be oriented by rotation on goniometer around an axis through the surface of the sample. The incidence angle is defined by the optical axis of the source arm and the normal to the surface of the sample.

Ellipsometry includes:

- **The source**: it is a short arc Xenon lamp at high pressure, of a very low residual polarization. It emits on the visible spectrum, from near ultraviolet to near infrared. The beam size (0.25 mm) from the arc, is collimated by a high focal length mirror to obtain a slightly divergent beam (0.3 mrad), which is necessary for a good definition of the incidence angle, and flatness of the incident wave.
- **The polarizer**: once collimated, the beam polarization is modulated by a rotating polarizer and low deviation with high extinction rates. It runs at a speed of 40 rounds per second.
- **The goniometer**: ellipsometry arms are mounted on a high-resolution double ring goniometer. The angular resolution is a key factor for the proper calibration of the instrument and its use in photometry.
- **Sample holder**: the sample is maintained by suction, (allows to limit all constraints on the surface of the holder), and adjustable following two directions. The orientation of the optical surface can be spotted using an autocollimator. The surface of the sample must be free of dust and oily traces.
- **Analyzer**: positioned after the sample, it is fixed during the measurement. After passing through the Analyzer, the beam is focused at the input of an optical fiber for the optical connection with the spectrometer.

- **The spectrometer**: it is mechanically independent from rotation block, for better handling. The beam at the output of fibre is focused on the slot of a Czerny-Turner spectrometer mirror of 500 mm focal length. The spectrometer consists of two additives dispersive elements separated by a fixed intermediate slit. The first part dispersive element is a prism dispersing spectrum on the intermediate slot. It acts as a filter of linewidth defined by the slot width and a center wavelength variable depending on the position of the Prism. The isolated spectral bandwidth is then dispersed in the second part through a higher order grating, allowing a high spectral resolution. The Prism ensures the selection of the grating order.
- **The photomultiplier**: the detector is a photomultiplier working from the ultraviolet to the near infrared.

Finally the spectroscopic ellipsometry found its applications in areas involving thin films or surface analysis such as:

- Optics: characterization of thickness and refractive index of dielectrics and metals used in the fabrication of mirrors, anti-reflective layers and polarizing surfaces;
- Solid-state physics: measurement of permittivities which characterize crystallinity or the amorphization state of a material, semiconductor element band structure, or the coating of a deposited layer (polymer), porosity (by determining the concentration of the vacuum in the material).

2.6 Conclusion

In the first part of this chapter we have presented the synthesis method of titanium dioxide layers. In addition and in order to facilitate the identification of TiO_2 thin films, we presented the main techniques to perform electrical, structural, morphological and optical characterizations of these films. The second part was devoted to the description of a gas sensor set-up and to the principles of optical and optoelectronic measurements.

References

1. Saminadayar K (1997) Cours de Physique des couches minces, Formation doctorale Microélectronique
2. Chatterjee S (2008) Titania-germanium nanocomposite as a photovoltaic material. Sol Energy 82:95
3. Brundle CR, Evans CA, Wilson S (1992) Encyclopedia of materials characterization—surfaces, interfaces, thin films. Elsevier, Amsterdam, p 800
4. Patterson AL (1939) The scherrer formula for x-ray particle size determination. Phys Rev 56:978
5. Bejoui A (2009) Etudes électriques, structurales et morphologiques des oxydes de cuivre (Cu_2O, CuO) pour l’application capteur. Mastère, Institut National des Sciences appliquées et de Technologie

6. Selvan JAA (1998) Thèse docorat, Université de Neuchâtel. ISBN 3-930803-60-7
7. Adachi A (1982) J Appl Phys 53:8775
8. Labidi A, Bejaoui A, Ouali H, Akkari FC, Hajjaji A, Gaidi M, Kanzari M, Bessais B, Maaref M (2011) Appl Surf Sci 257:9941
9. Dimassi W (2007) Etudes spectroscopiques et optoélectroniques de la passivation des cellules solaires au silicium multicristallin basée sur l'élaboration du silicium poreux. Thèse doctorat, Faculté de Sciences de Tunis
10. Honsberg C, Bowden S (1998) Photovoltaics: devices, systems and applications (CDROM). University of New South Wales, Sydney

http://www.springer.com/978-3-319-13352-2

Chromium Doped TiO_2 Sputtered Thin Films
Synthesis, Physical Investigations and Applications
Hajjaji, A.; Amlouk, M.; Gaidi, M.; Bessais, B.; El Khakani, M.A.
2015, XIII, 86 p. 77 illus., 11 illus. in color., Softcover
ISBN: 978-3-319-13352-2